Structural Characterization of the Micelle-Vesicle Transition in Lecithin-Bile Salt Solutions

Michelle A. Long,* Eric W. Kaler,* and Sum P. Lee‡
*Center for Molecular and Engineering Thermodynamics, Department of Chemical Engineering, University of Delaware, Newark, Delaware 19716; and ‡Veterans Administration Medical Center, Seattle, Washington 98108 USA

ABSTRACT Small-angle neutron scattering (SANS) and dynamic light scattering (QLS) are used to characterize the aggregates found upon dilution of mixed lecithin-bile salt micelles. Molar ratios of lecithin (L) to taurocholate (TC) studied varied from 0.1 to 1, and one series contained cholesterol (Ch). Mixed aggregates of L and taurodeoxycholate (TDC) at ratios of 0.4 and 1 were also examined. In all cases the micelles are cylindrical or globular and elongate upon dilution. The radius of the mixed micelles varies only slightly with the overall composition of lecithin and bile salt which indicates that the composition of the cylindrical micelle body is nearly constant. The transition from micelles to vesicles is a smooth transformation involving a region where micelles and vesicles coexist. SANS measurements are more sensitive to the presence of two aggregate populations than QLS. Beyond the coexistence region the vesicle size and degree of polydispersity decrease with dilution. Incorporation of a small amount of cholesterol in the lipid mixture does not affect the sequence of observed aggregate structures.

INTRODUCTION

Along the physiological pathway of bile, cholesterol is alternately solubilized by lecithin vesicles and lecithin-bile salt mixed micelles. At a low bile salt secretory rate, lecithin-rich vesicles become the major cholesterol carriers in hepatic bile (Lee et al. 1987). Between meals hepatic bile is diverted to the gallbladder for storage. During storage in the gallbladder, bile is concentrated and the vesicles transform into mixed lecithin-bile salt micelles. After a meal, the gallbladder empties, and dilution of bile upon entering the intestine causes the micellar cholesterol carriers to revert to lecithin-rich vesicles. The intermediate structures formed during the micelle-vesicle transition, and the vesicles themselves, are believed to be important substrates for effective enzyme activity during breakdown of phospholipids and triglycerides for intake by the body (Hofmann and Mysels, 1988).

Knowledge of the structural transitions and the forces that drive them from a thermodynamic standpoint is necessary to guide understanding of mechanisms of enzyme activity in the intestine, protein reconstitution in model membranes, or cholesterol nucleation and gallstone growth in the gallbladder. Much research to date has focused on the effects of surfactant concentration, the relative composition of surfactant mixtures, and the aggregative properties of individual surfactants on the vesicle-to-micelle transformation. These studies have used various experimental techniques including turbidity measurements (Almog et al., 1986, 1990; Lichtenberg et al., 1979), static and dynamic light scattering (Almog et al., 1986, 1990; Mazer et al., 1980, 1984, Schurtenberger et al., 1985, Stark et al., 1985), fluorimetry (Almog et al., 1990; Reda and Spink, 1987, Schubert and Schmidt, 1988) and NMR (Almog et al., 1990; Lichtenberg et al., 1979, Stark et al., 1983, 1985). Experimental determination of the aggregate structure has also been attempted by small-angle neutron scattering (Hjelm et al., 1988, 1990, 1992), small angle x-ray scattering (Muller, 1981) and cryo-transmission electron microscopy (Vinson et al., 1989, Walter et al., 1991).

The focus of this paper is determination of the progression of aggregate structures that occur on dilution of a concentrated lecithin-bile salt solution. Mechanistic descriptions of this transition in lecithin-bile salt solutions have relied mainly on the "mixed disk" model of the micelle structure (Mazer et al., 1980). This model successfully describes the increase of the apparent hydrodynamic radius, as measured by dynamic light scattering, of the micelles with dilution. Along a dilution path the apparent hydrodynamic radius initially increases to a maximum size and then decreases with further dilution. This increase in size is interpreted in terms of the mixed disk model as radial growth of disk-shaped micelles. In this view, a bilayer of lecithin interspersed with dimers of bile salt forms the body of the disk while a ring of bile salt surrounds the perimeter of the micelle body and reduces the unfavorable exposure of the lecithin hydrocarbon tails to the external aqueous solution. Dilution of the micelle solution leaches bile salt from the micelles to maintain an intermicellar monomer concentration (IMC). The disks coalesce to balance the remaining bile salt with the total area of exposed edges. The disk micelles are postulated to continue to grow in this fashion upon dilution until there is no longer sufficient bile salt to stabilize the edges. At this point the large disks or sheets are assumed to fold spontaneously into vesicles, and the apparent hydrodynamic radius decreases.

Received for publication 11 August 1993 and in final form 20 July 1994.
Address reprint requests to Dr. Eric W. Kaler, Department of Chemical Engineering, University of Delaware, Newark, DE 19716-3119. Tel.: 302 831 3553; Fax: 302 831 4466; E-mail: kaler@che.udel.edu.
Abbreviations used: L - egg yolk lecithin, BS - bile salt, L/BS - molar ratio of lecithin to bile salt, TC - taurocholate, TDC - taurodeoxycholate, Ch - cholesterol, SANS - small-angle neutron scattering, QLS - quasielastic light scattering, cryo-TEM - cryo-transmission electron microscopy, D_2O - deuterium oxide, IMC - intermicellar concentration, RPA - Random phase approximation

0006-3495/94/10/1733/10 $2.00

Small-angle neutron scattering studies have since shown that in concentrated solutions lecithin-bile salt aggregates are not disks, but cylindrical micelles (Hjelm et al., 1988, 1990, Long, 1993, Long et al., 1994) in which the lecithin molecules are oriented radially along the aggregate axis and the bile salt molecules lay flat at the interface (Hjelm et al., 1992, Nichols and Ozarowski, 1990). Upon dilution, these micelles first elongate, then apparently form large lamellar sheets that ultimately fold to form unilamellar vesicles. Elongated micelles have been directly observed using cryo-transmission electron microscopy following the dissolution of lecithin vesicles by addition of sodium cholate (Walter et al., 1991). Though the micelle shape in the original mixed disk model is in error, the idea that growth follows the extraction of the more soluble surfactant is attractive and probably correct. Rewriting the model in terms of elongational growth of the micelles, as opposed to radial growth, predicts the same increase of the apparent hydrodynamic radius (Nichols and Ozarowski, 1990).

Here we report the results of small-angle neutron scattering and dynamic light scattering measurements of lecithin-bile salt mixtures in aqueous solution. From these data we obtain quantitative information about the structure and composition of lecithin-bile salt aggregates. The transition from micelle to vesicle is monitored as a function of the lecithin to bile salt molar ratio, the amount of cholesterol, the total lipid concentration, and type of bile salt. The micelle to vesicle transition is continuous with a region near the micellar phase boundary over which micelles and vesicles coexist. The findings reported here closely parallel those obtained from cryo-transmission electron microscopy images of vesicle dissolution by sodium cholate (Walter et al., 1991).

MATERIALS AND METHODS

Materials

Egg yolk lecithin (received in chloroform or hexane), sodium taurocholate (TC), sodium taurodeoxycholate (TDC), and cholesterol were obtained from Sigma Chemical Company (St. Louis, MO). All lipids were of analytic grade and were used as received.

Solutions

Solutions of lecithin and the appropriate bile salt were made using the method of coprecipitation (Almog et al., 1990). Lecithin and bile salt were dissolved in a methanol/chloroform mixture, and the solution was dried under nitrogen in a rotating scintillation vial to produce a thin film. These films were further dried under vacuum until they reached a constant dry weight (typically 4 to 5 days). For samples containing cholesterol, the cholesterol was dissolved in chloroform and added to the lecithin-bile salt solution before drying. Appropriate amounts of D_2O saline solution (0.15 M NaCl) were added to make stock solutions of 5 g/dl total lipid. The 5 g/dl concentration includes cholesterol when it is in the sample, and the molar ratios for such samples are given as (L + Ch)/BS. These stock solutions were diluted to the final concentrations used in the experiments, and all samples were sealed under argon and stored at 25°C for at least two days. This procedure has been shown to be sufficient to prevent degradation of the lecithin for several weeks (Little et al., 1993). All stock solutions for light scattering were filtered through Gelman 0.22 μ Acrodisk-13 filters. Dilutions were made with similarly filtered saline solutions. These samples were sealed under argon in 5 ml acid-washed ampules.

To construct the L-TC-H_2O phase diagram, lecithin films were made as above in 2 ml screw cap vials. After achieving a constant dry weight the appropriate amounts of saline and dry bile salt were added. Phase observations were recorded over a period of four weeks.

Methods

Light scattering measurements were made using a home built apparatus (Douglas and Kaler, 1991) employing a Langley-Ford model 1080 correlator and a 2W Lexel Ar^+ laser operated at 488 nm wavelength. The measured autocorrelation functions were analyzed for the first and second cumulant of a cumulant fit (Koppel, 1971). The first cumulant provides an estimate of the apparent diffusion coefficient and the second cumulant is a measure of the polydispersity. The data are reported in terms of the spherical equivalent hydrodynamic radius using the Stokes-Einstein equation

$$R_h = kT/6\pi\eta D, \quad (1)$$

where k is the Boltzmann constant, T is the temperature (25°C), η is the solvent viscosity, and D is the diffusion coefficient obtained from the first cumulant.

Small-angle neutron scattering measurements were made at the Oak Ridge National Laboratory (ORNL, Oak Ridge, TN) and the National Institute of Standards and Technology (Gaithersburg, MD). The samples were measured in quartz cells of 0.2 cm pathlength using neutrons with wavelengths (λ) of either 4.75 Å or 7 Å. Background contributions of the solvent and any residual instrument background scattering were subtracted from the measured scattering curves. The intensities were placed on an absolute scale using standards supplied by the neutron facilities. The scattered intensity is reported in terms of the magnitude of the scattering vector $q = 4\pi/\lambda \sin(\theta/2)$ where θ is the scattering angle. The procedures used to analyze the data are given in the Appendix.

RESULTS AND ANALYSIS

The structural transitions of lecithin-bile salt mixtures are observed as a function of the total surfactant concentration, ratio of lecithin to bile salt (L/BS), the type of bile salt (taurocholate (TC) or taurodeoxycholate (TDC)), and the concentration of cholesterol. The samples are made by diluting 5 g/dl total lipid stock solutions of a given overall molar ratio of lecithin and bile salt. Depending on the bile salt species and the concentration of cholesterol, these stock solutions range from about 77 to 90 mM. At high water contents, the dilution paths approach, but do not cross, the equilibrium phase boundary that separates the isotropic micellar region and a two-phase region that consists of a clear inviscid upper phase and precipitated bilayers (Fig. 1). No precipitated lamellar phases appeared in the samples prepared for the scattering experiments.

The apparent hydrodynamic radius measured by dynamic light scattering of equimolar lecithin and taurocholate samples (Fig. 2) shows the expected increase in size with dilution. The maximum apparent radius is approximately 500 Å at a concentration of 12.8 mM. Beyond this transition point both the apparent particle size and the polydispersity, as determined from the second cumulant (not shown), decrease. The measured correlation function of the 4x dilution (19.1 mM) is best fit by a double exponential decay, which suggests the presence of a bimodal population of aggregates. The hydrodynamic radii calculated from the fits to the neutron data (Eqs. A.9 and A.10) are also included in Fig. 2. Measurements along dilution paths for other ratios of L/TC are

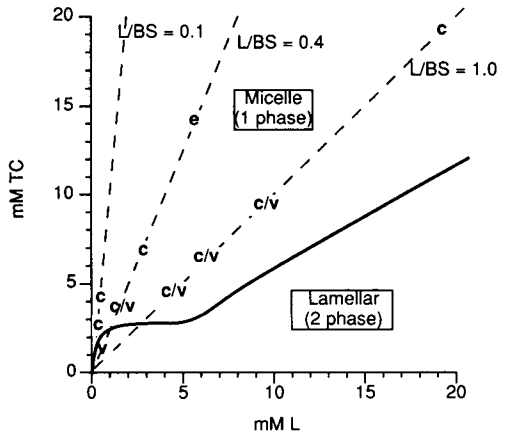

FIGURE 1 L-TC-H_2O equilibrium phase diagram (> 97.5 wt% water). The phase boundary between the isotropic micellar region and the two phase lamellar region is marked by the solid line. Dashed lines indicate the dilution paths sampled in the scattering experiments. Aggregate shapes found in different regions of the phase diagram are plotted where e = ellipsoidal micelles, c = cylindrical micelles, c/v indicates where micelles and vesicles coexist, and v = vesicles.

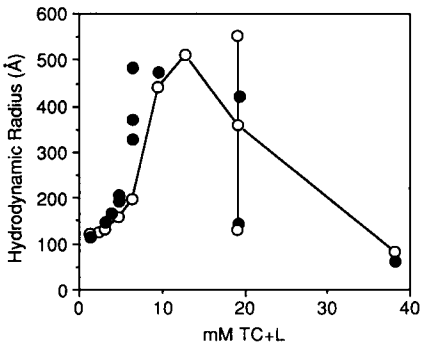

FIGURE 2 Hydrodynamic radius as a function of total lipid concentration for L/TC = 1 as measured by dynamic light scattering (open circles) and calculated from the fits to the neutron data (filled circles). The autocorrelation function of the 19.1 mM sample was best fit by a double exponential function and the resulting hydrodynamic radii are 130 Å and 550 Å.

similar. The maximum apparent particle size occurs at lower concentrations as the lipid ratio decreases and is 6.50 mM for L/TC = 0.8 and 4.14 mM for L/TC = 0.4. The hydrodynamic radius of the L/TDC = 1 series peaks at a much lower total lipid concentration of 1.72 mM.

After 48 h of equilibration, further dilution of samples that are already at or beyond the maximum particle size does not produce any change in the aggregate size, in agreement with previous reports (Schurtenberger et al., 1985). Further, it was observed that dilution of a concentrated micellar solution (L/TC = 0.8, 26.0 mM, R_h = 60 Å) reproduces the aggregate sizes of the original dilution path. However, dilution of a less concentrated micellar sample (13.0 mM, R_h = 140 Å) of the same series gives aggregates with R_h = 400 Å, but they do not produce the anticipated decrease in size at lower concentrations.

The small-angle neutron scattering (SANS) spectra plainly illustrate the evolution of the aggregate morphology with dilution. For these experiments, dilution series were made along the paths L/TC = 0.1, 0.4, 1, and L/TDC = 0.4 and 1. An additional series of L/TC = 0.4 with 10% cholesterol was also measured. All samples for neutron scattering were made by direct dilution of 5 g/dl stock solutions with no intermediate equilibration steps. Fig. 3 shows the scattering curves of the dilution series with molar ratio L/TC = 1 (initial concentration 76.5 mM). The scattering spectra of this series shows a transition from monotonic curves at high surfactant concentrations to spectra exhibiting distinct maxima and minima in the most dilute samples. The series of L/TC = 0.1, 0.4, and L/TC = 0.4 containing 10% cholesterol show the same progression of scattering spectra.

The scattered intensity patterns of most solutions within the micelle region of the phase diagram exhibit the characteristic 1/q dependence of cylindrical micelles at intermediate values of q. The 20.7 mM samples of the L/TC = 0.4 series with and without cholesterol do not, however, and are best fit as ellipsoidal micelles. Initial interpretation of the micelle spectra begins with the modified Guinier analysis (see Appendix). Fig. 4 shows the modified Guinier plots of the intensity/gram surfactant for the L/TDC = 1 series. At

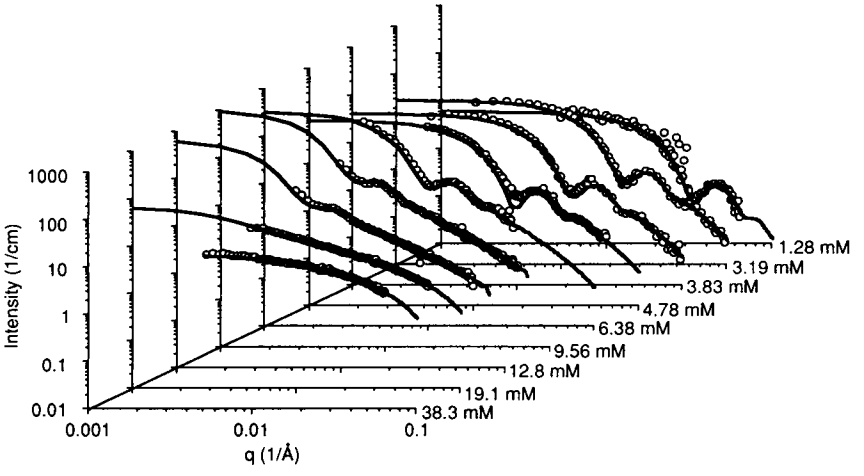

FIGURE 3 Small-angle neutron scattering of a serial dilution of an equimolar 5 g/dl (76.5 mM) lecithin-taurocholate solution. The solid lines are the fits to the data as described in the text.

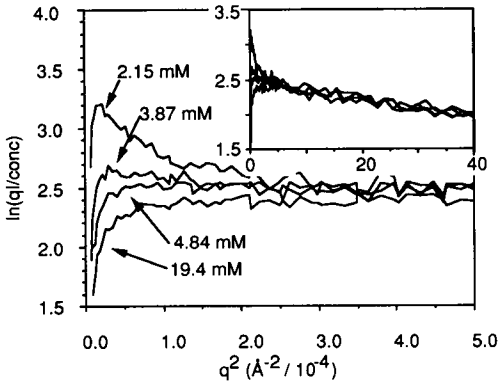

FIGURE 4 Modified Guinier plots of the spectra from samples with L/TDC = 1. The curves increase at low q sequentially with dilution. The shape of the curves of the 19.4 to 3.87 mM samples are characteristic of rigid cylindrical particles of finite length. The peak at low q for higher dilutions suggests the presence of bilayer structures. The inset shows the same plot over a larger q-range.

high q (inset of Fig. 4), the spectra collapse to a common profile. This implies that the micelle radius is approximately constant with total surfactant content. The apparent radius determined from the slope of the curve in this region is constant as the concentration decreases from 4.78 to 2.73 mM (Table 1). On the other hand, the apparent radius of the most concentrated samples of the L/TC = 0.4 and L/TC = 1 series increases markedly with dilution over a smaller concentration range, and the high q region of the modified Guinier plots for the most concentrated samples with L/TC = 0.4 do not overlay one another (not shown). The lower radius of the ellipsoidal micelles is consistent with the limitation of the modified Guinier approximation for particles of finite length (Hjelm, 1985).

Qualitative information about the length of the particles is obtained from the low q portion of the modified Guinier plot. The magnitude of the low q portion of the curve increases with decreasing concentration. This increase is consistent with both increasing micelle length and the lessening of interparticle interactions. The maximum of each curve indicates the point where the scattering experiment probes distances within the solution that are less than 1/L. The fact that the maximum moves to lower q with decreasing concentration is again consistent with particle growth. The shape of the curves of Fig. 4 for samples from 19.1 to 3.83 mM is consistent with that expected for a rigid cylindrical particle. The curve increases with q and then smoothly turns over and decays linearly, with a constant slope, to the highest q measured. The intensity of the most dilute sample (2.13 mM) also increases with q at low q, but then decreases in two stages. The initial intensity decrease is steep, and it then levels out to parallel the high q regions of the other curves. This behavior has been associated with flexible cylindrical micelles (Marignan et al., 1989), and is also observed for the L-TC samples that contain both micelles and vesicles.

The micelle dimensions determined from the fits to the entire spectra are given in Table 2. All spectra in the series L/TDC = 0.4 are well fit to the scattering model for cylindrical micelles (Fig. 5). The most dilute sample in this series has a concentration of 0.75 mM TDC and 0.3 mM L (80x dilution). The estimated IMC, calculated as described in the Appendix, is included in Table 2. The IMC decreases with overall surfactant concentration, and the IMC of TC is higher than that of the more hydrophobic TDC.

For the lecithin-taurocholate mixtures, a maximum appears in the scattering curve when the sample concentration is close to the phase boundary. In this case, the maximum indicates the appearance of vesicles, however, the scattering data at $q > 0.04$ Å^{-1} show the characteristic 1/q dependence of cylindrical particles. For samples in this region, the data are fit by assuming the measured scattered intensity is the sum of the intensity of a population of both cylindrical micelles and vesicles (Eq. A.7, Table 3). Although no maximum is readily apparent, the 19.1 mM sample of the L/TC = 1

TABLE 1 Apparent cylindrical radius from modified Guinier analysis

Molar-ratio L/BS	Concentration (mM)	Radius (Å)
L/TC = 0.1	2.99	24.2 (2.2)
	2.49	25.6 (2.9)
L/TC = 0.4	20.7	19.4 (0.6)
	10.4	23.6 (0.4)
	6.90	27.9 (0.4)
L+Ch/TC = 0.4	10.6	25.8 (0.9)
L/TC = 1	38.3	22.3 (1.5)
	19.1	24.7 (0.6)
	12.8	26.1 (0.3)
L/TDC = 1	19.4	20.6 (0.7)
	4.84	25.8 (0.5)
	3.87	24.5 (1.2)
	3.22	26.8 (0.9)
	2.76	26.1 (1.0)

The radii obtained from the modified Guinier plot are apparent dimensions that have not been corrected for the distribution of scattering lengths within the aggregate.

TABLE 2 Micelle dimensions and IMCs derived from fits to SANS data

Molar ratio L/BS	Concentration (mM)	Radius (Å)	Length (Å)	IMC (mM)
L/TC = 0.1				
	4.48	24	110	3.1
	2.99	24	700	2.6
	2.49	24	700	2.1
L/TC = 0.4	20.7*	25	35	
	10.4	22	105	5.2
L+Ch/TC = 0.4	21.1*	25	35	
	10.6	21	125	
L/TC = 1	38.3	22	280	4.9
L/TDC = 0.4	21.1*	20	25	
	4.22	20	50	2.1
	1.69	20	75	1.0
	1.41	20	100	0.97
	1.20	20	100	0.76
	1.05	20	150	0.74

* Prolate ellipsoid. The dimensions given are the semi-minor and semi-major axes.

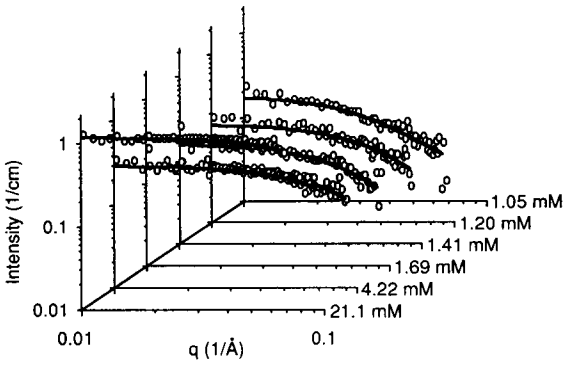

FIGURE 5 Small-angle neutron scattering of a serial dilution of a 5 g/dl (84.3 mM) lecithin-taurodeoxycholate solution with a molar ratio of 0.4. The solid lines are the fits to the data as described in the text.

TABLE 3 Mixed micelle*-vesicle‡ samples in L/TC = 1 series

Concentration (mM)	Number of micelles as of aggregate population	IMC (mM)
19.1	99%	
12.8	68%	2.9
9.56	24%	3.0

* Micelle apparent radius 22 Å length 800 Å.

‡ The outer vesicle radius is fit to 462 Å assuming a bilayer thickness of 32 Å. The SD of the radius is 100 Å and represents the spread of the vesicle size, not an error estimate for the parameter.

series is also best fit by assuming a mixture of vesicles and micelles. The samples containing both micelles and vesicles are plotted in Fig. 1. The larger radii and long micelle lengths of the fits to the three most concentrated samples of the L/TC = 0.1 series might also reflect the presence of vesicles, but the spectra of these samples do not have the low q data necessary to distinguish the signature scattering from vesicles.

With the average scattering length density of the vesicles, one can estimate the amount of surfactant distributed between the micelles and vesicles in the samples in which the aggregates coexist. The only free parameter in A_v is ϕ_v, the volume fraction of lecithin in the vesicle, so fitting the data allows determination of the volume fraction of the micelles. The percentage of surfactant found in the micelles is given in Table 3. The relative number of vesicles in solution increases at the expense of the micelles with decreasing surfactant concentration.

Beyond the region of micelle-vesicle coexistence, the intensity over the entire q range can be successfully fit to a model of polydisperse vesicles (Fig. 6). The best fit of the bilayer width is 32 Å. The vesicle size and degree of polydispersity are not affected by the presence of cholesterol. In general, the size and degree of polydispersity decrease with dilution, in agreement with the dynamic light scattering measurements (Fig. 2). Other comments on these scattering curves are given in the Appendix.

Reproducible time-dependent changes were observed during the SANS experiment for samples near the phase boundary. Fig. 7 shows the time progression of the scattering from

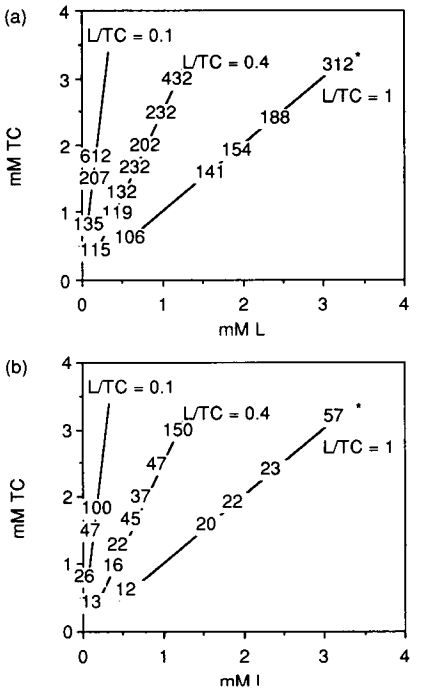

FIGURE 6 (a) Fitted vesicle radius and (b) standard deviation, both in unit of Å. Both the size and degree of polydispersity of the vesicles decreases with the total surfactant concentration. The sample indicated by * changed with time over the course of the experiment and was fit to 312 Å ± 57 Å and 482 Å ± 100 Å depending on the age of the sample. The L/TC = 0.4 series that included cholesterol have vesicle sizes of 460 Å ± 105 Å, 210 ± 50, 144 ± 23, 120 ± 17, and 113 ± 15 Å.

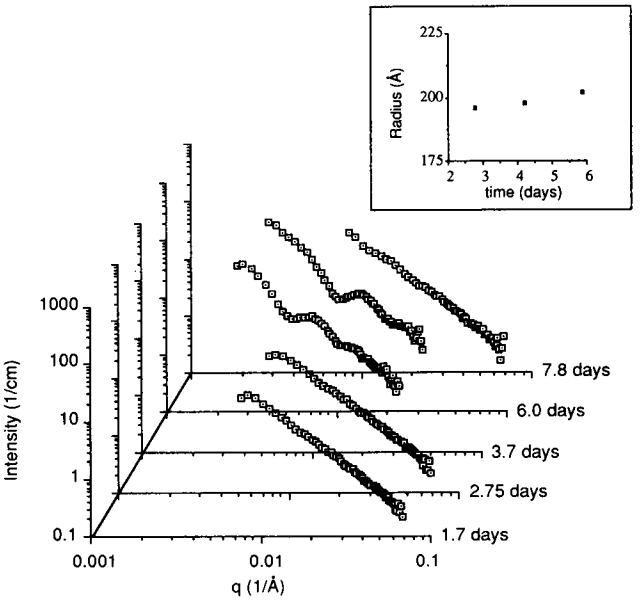

FIGURE 7 Time-dependent changes of the SANS spectra of a 6.38 mM solution of an equimolar mixture of lecithin and taurocholate. The inset shows the hydrodynamic radius measured by QLS which shows little change over the same period of time.

an equimolar L/TC sample at 6.38 mM. Initial measurement of the sample produced a featureless scattering curve with log I versus log q slope of -2, which is consistent with the

existence of sheet-like structures, including very large vesicles. Between 4 and 6 days distinct maxima and minima appeared that are fit to a model of polydisperse vesicles with an average radius of 302 Å ± 53 Å. Subsequent remeasurement 2 days later show no extrema in the scattered intensity, and the log I versus log q slope remains at -2. No significant variation of the size measured by dynamic light scattering is observed under the same conditions.

DISCUSSION

The structural transitions observed in the L-TC system are similar to those previously measured for mixtures of lecithin and glycocholate (Hjelm et al., 1988, 1990) where the micelles are ellipsoidal or globular at lecithin concentrations above 20 mM when L/BS < 1. The micelle length increases upon dilution for all lipid ratios studied. As the overall sample concentration approaches the micelle/lamellar phase boundary, polydisperse vesicles coexist with the micelles. With continued dilution, the size and degree of polydispersity of the vesicles decreases. The largest vesicles have radii of 400 Å to 600 Å, in agreement with the estimate of 500 Å for the vesicles of lecithin and sodium cholate measured by turbidity and electron microscopy (Almog et al., 1986). The smallest vesicles have radii of 115 Å to 140 Å, sizes consistent with predictions for the minimum size of pure lecithin vesicles (Brouillette et al., 1982). The fitted bilayer width of 32 Å is in line with previous estimates of the thickness of the hydrocarbon region of the bilayer that range from 29.5 Å to 37 Å (Small, 1967, Cornell et al., 1980).

The structures determined from the SANS data correspond well to the cryo-transmission electron microscopy (cryo-TEM) images of lecithin and sodium cholate aggregates (Walter et al., 1991). The minor discrepancies are attributed to the fact that the cryo-TEM experiments followed the dissolution of vesicles by addition of cholate, and the sequence of formation of the various surfactant aggregates probably differs from the reverse process followed here. At high total lecithin and bile salt concentrations Walter and co-workers observed small mixed micelles similar to the ellipsoidal micelles found here and reported elsewhere (Müller, 1981). With decreasing cholate content an isotropic solution of extremely long (2000 Å - 3000 Å) and flexible micelles was found. Micelles of this length are not observed here, but may be present in the region where micelles and vesicles coexist. Reliable determination of the cylinder length by SANS is not possible in the presence of large vesicles. The coexistence of cylindrical micelles with lecithin vesicles was observed in the cryo-TEM pictures at 9 mM lecithin with cholate concentrations between 6 mM and 7.25 mM (Walter et al., 1991). Dynamic light scattering measurements confirm the presence of two populations of aggregates (Fig. 2) in a mixture of 9.6 mM TC and 9.6 mM L. The more dilute samples of the L/TC = 1 series (9.6 mM and 12.8 mM total lipid) do not exhibit signs of a bimodal population in the QLS measurements, even though two aggregate shapes are observed in the SANS data (Fig. 3). This suggests that the micelles are long enough that the diffusion coefficient of the micelles is indistinguishable from that of the vesicles. For example, a cylindrical micelle with an apparent hydrodynamic radius of 450 Å would have a length of approximately 4000 Å, in line with the dimensions established by the cryo-TEM measurements.

SANS spectra from samples containing both micelles and vesicles can be misinterpreted. The coexistence of vesicles and micelles interferes with the usefulness of the modified Guinier plot to obtain structural information about the aggregates. Although these spectra exhibit the 1/q dependence of cylindrical micelles at high q, the contribution of the vesicles to the scattering causes the cross-sectional radius of gyration obtained from the slope to increase as the number of vesicles increases. This effect is especially evident for the L-TC samples that undergo the micelle-vesicle transition at much lower concentrations than do the samples made of L and TDC. The maxima and minima characteristic of vesicle scattering do not appear in the L/TDC = 1 scattering curves until the total surfactant concentration is less than 1.8 mM, but evidence for the presence of vesicles before this point is seen in the modified Guinier plot (Fig. 4). As the concentration decreases the curves show an initial steep decrease that levels out to parallel the slope of the plots for the more concentrated samples. This same behavior is observed for the L-TC samples with coexisting micelles and vesicles. The upturn occurs because the asymptotic intensity scattered by vesicles goes as q^{-2} instead of the q^{-1} dependence of the scattered intensity of cylindrical micelles. The spectra of flexible coils also go as q^{-2} (Kratky, 1982), and a similar upturn in the modified Guinier plot of the scattered intensity of cetylpyridinium bromide micelles has been attributed to micelle flexibility (Marignan et al., 1989). It is not possible to determine unambiguously whether the upturn is caused by vesicles or flexible micelles in the L-TDC samples. The samples may contain both structures as suggested by the cryo-TEM images (Walter et al., 1991).

By fitting the entire q-range of the scattered intensity on absolute scale, the SANS data provide information about the distribution of surfactant between the aggregates that is not available from the cryo-TEM technique or light scattering. The transitions from micelles to vesicles occur as the bile salt is redistributed between the micelles and the aqueous solution. The concentration of bile salt in the micelles decreases with dilution because bile salt must maintain an external monomer concentration (the IMC). The simplest view is that the micelles consist of a mixed surfactant body capped on the ends by bile salt. Upon dilution bile salt is extracted from the ends to maintain the IMC, while the composition of the body remains constant (Nichols and Ozarowski, 1990). Thus the micelles grow with dilution, and the overall composition of a micelle varies as the micelle length changes, with lower L/BS ratios in shorter micelles. This simple mechanism suggests that the cylindrical structure persists until there is no longer sufficient bile salt to maintain the L/BS ratio in the cylinder body. At this point the aggregates transform into vesicles or bilayer sheets. This mechanism is supported by the data presented here. The transformation occurs gradually

and the population of vesicles increases as the number of micelles decreases. This process is similar to the phase separation of lecithin-octyl glucoside mixtures into a distinct vesicle phase and a separate micellar phase (Almog et al., 1990). It is important to note that the micelle-vesicle coexistence in lecithin-bile salt solutions is not true phase separation, thus complicating quantitative analysis of the partitioning of bile salt between the aggregates.

Qualitative information about the composition of the cylindrical micelles is obtained from the fitted dimensions. The scattering spectra of the cylindrical L-TDC micelles are fit to an apparent radius of about 20 Å that is constant with changing surfactant concentration. The L-TC micelles are fit using an apparent radius of roughly 22 Å for both the L/TC = 0.4 and L/TC = 1 series. Because the radius of a mixed micelle will depend on composition when the two surfactant components have unequal hydrocarbon tail lengths (Szleifer et al., 1987), the constant micelle radius indicates that the micelle body composition does not change with overall surfactant concentration or lipid composition. In addition, the micelle length increases with dilution, reflecting the overall increase of L/BS within the micelle as bile salt is extracted to maintain the IMC. The calculated IMC values decrease with decreasing concentration as observed previously for lecithin-bile salt mixtures (Duane, 1975, 1977, Shankland, 1970). The IMC of TC is reported to lie between 2 mM and 5 mM for less than ~15 mM total lipid (Nichols and Ozarowski, 1990, Duane, 1977, Donovan et al., 1991), and the IMC of TDC varies from 0.55 mM to 3 mM (Nichols and Ozarowski, 1990, Borgström, 1978). Both values are in agreement with those in Table 2. The IMC represents both the free monomer concentration and the concentration of bile salt forming simple micelles when the IMC is greater than the CMC of the bile salt. (The SANS of simple micelles is expected to be negligible compared to that of the mixed micelles and is not considered here.)

The vesicle spectra are rigorously fit to a model of lecithin vesicles free of bile salt. The scattering arises only from the tail region, so the head group region must be highly hydrated. A model for the vesicles that provides the composition of the head group layer (which would include both bile salt molecules and waters of hydration) requires high quality data at high values of q, but the results of the modeling presented here indicate that it is unlikely that a significant amount of bile salt resides in the center of the vesicle bilayer. Instead, the variation in size of the vesicles formed by dilution is better described by a recently proposed mechanism relating the vesicle size and polydispersity to the rate of bile salt extraction from the bilayer (Rotenberg and Lichtenberg, 1991). In this case immediate dilution of a concentrated micellar solution results in small vesicles because of the rapid extraction of bile salt from the membrane. However if the surfactant solution is diluted in a series of steps with intermediate equilibration, the concentration gradient responsible for extraction of bile salt is smaller. This allows bile salt in the membrane more time to swell the bilayer which results in larger vesicles.

Fig. 7 shows that some of the structural transitions are slow and can take at least a week to reach a steady state. Within this time frame QLS measurements show no apparent change in particle size. These transitions are not due to degradation of the lecithin because no transitions are observed for micelle or vesicle samples over the same time period, and independent measurements have shown no lecithin degradation in samples prepared using our methods (Little et al., 1993). This result emphasizes that caution should be maintained in deriving complicated structural models from dynamic light scattering alone. Similarly, the peak of the hydrodynamic radius with dilution measured by dynamic light scattering has long been associated with the micelle-vesicle phase boundary (Mazer et al., 1980), however, the mixed micelle-vesicle samples measured by SANS appear well before this boundary.

Overall, the interpretation of the SANS data presented here is consistent with recent reports of the mixed lecithin-bile salt aggregate structures. The micelle radius obtained from the fit to the full scattering spectra of the micelles varies only slightly with the overall composition of lecithin and bile salt indicating a constant composition of the cylindrical micelle body. Micelle growth occurs as the surfactant concentration approaches the micelle phase boundary. The transition from micelles to vesicles is smooth and involves a region where micelles and vesicles coexist. Beyond the coexistence region the vesicle size and degree of polydispersity decrease with dilution. Incorporation of a small amount of cholesterol in the lipid mixture does not affect the size or the sequence of appearance of aggregate structures. Similar aggregates are found in mixtures containing lecithin and either TC or TDC, however vesicles do not appear in the mixtures containing the more hydrophobic bile salt TDC until much lower surfactant concentrations.

CONCLUSION

Small-angle neutron scattering is a powerful tool for elucidating the details of aggregate structure found in lecithin-bile salt mixtures. The results here show a continuous transition from cylindrical micelles to unilamellar vesicles. A region of micelle-vesicle coexistence, observed when solubilizing vesicles with sodium cholate (Walter et al., 1991), is also found in the reverse pathway. The changes in vesicle size with time are consistent with the proposed mechanism for vesicle formation that details the importance of the kinetics of detergent partitioning between the aqueous solution and the vesicles (Rotenberg and Lichtenberg, 1991).

The effect of cholesterol on the micelle to vesicle transition is minimal at the low cholesterol concentrations used here. This justifies study of the behavior of lecithin-bile salt mixtures as models for more complex lecithin-bile salt-cholesterol mixtures. Further investigations at higher cholesterol contents would provide information about how cholesterol is carried in the micelle and would be helpful in understanding the mechanism of protein-enhanced cholesterol transfer from micelles to vesicles that preceeds cholesterol nucleation (Groen et al., 1989).

The dependence of the transitions on the micelle-lamella phase boundary points to the importance of the properties of the solubilizing surfactant in achieving the structural changes. The more informative structural information provided by the SANS measurements in comparison to the model-dependent interpretation of dynamic light scattering results emphasizes the need for caution in developing detailed models of particle growth and polydispersity based on hydrodynamic measurements alone.

Supported in part by the Division of Materials Sciences, U.S. Department of Energy, under contract DE-AC05-84OR21400 with Martin Marietta Energy Systems, Inc. We also acknowledge the support of the National Institute of Standards and Technology, U.S. Department of Commerce, in providing some of the facilities used in this experiment. This material is based in part upon activities supported by the National Science Foundation under Agreement DMR-9122444. We are grateful for the experimental help of G. D. Wignall, C. Glinka, and J. Barker.

This research was also supported in part by the Whitaker Foundation and by grant DK-41678 from the National Institutes of Health. Dr. Sum P. Lee is supported in part by the Medical Research Service of the Department of Veterans Affairs.

APPENDIX: ANALYSIS OF SCATTERING DATA

In a small angle scattering experiment the measured intensity on absolute scale represents the average scattering cross-section per unit volume and has units of cm^{-1}. The q-dependence of the intensity results from the spatial distribution of the scattering centers in solution. For many dilute surfactant solutions the intensity can be calculated as the product of two distinct functions of q that separate the intra- and inter- particle distribution of scattering centers. The measured intensity $I(q)$ is then

$$I(q) = N_p P(q) S(q), \tag{A1}$$

where N_p is the number density of particles. The function $S(q)$ accounts for the effects of interparticle interactions on the intensity. Interparticle interactions, such as electrostatic repulsions or excluded volume interactions, cause a non-random distribution of the particles in solution. Repulsive interactions lower the intensity measured at low values of q. With increasing q, $S(q)$ oscillates around a value of 1. When the interparticle interactions are negligible, $S(q) \sim 1$ for all q, and the intensity depends on the function $P(q)$ alone.

$P(q)$ is the intraparticle shape function, and describes the influence of the particle size, shape and internal structure on the scattering curve. The magnitude of $P(q)$ is a function of the scattering length density distribution within a particle. The scattering length density is given by $\rho(r) = \sum n_i b_i / V$, where n_i is the number of atomic elements in the region of volume V and b_i is the associated scattering length (Bacon, 1975). If the scattering length density is constant throughout the particle, then the product of the particle volume and the scattering length density difference, $\Delta\rho = (\rho - \rho_{sv})$, is factored out of the expression for $P(q)$ and

$$I(q) = N_p(\Delta\rho)^2 V_p^2 \tilde{P}(q) S(q) = (\Delta\rho)^2 \phi V_p \tilde{P}(q) S(q) = A\tilde{P}(q)S(q), \tag{A2}$$

where ϕ is the particle volume fraction. The function $\tilde{P}(q)$ is normalized to unity at $q = 0$, and the absolute magnitude of the intensity depends on the prefactor $A = (\Delta\rho)^2 \phi V_p$.

Small-angle neutron scattering

All of the intensity spectra are fit by assuming a constant scattering length density throughout the surfactant-containing portions of the vesicles and micelles. The expressions for the shape functions considered in this paper are listed in Table 4. The model parameters are fit using a least-squares error criterion to reproduce both the absolute magnitude and q-dependence of the measured data.

The lecithin-bile salt mixed micelles are either ellipsoidal or cylindrical in shape. The modified Guinier equation (Porod, 1982)

$$I(q) = \frac{A}{qL} \exp\left(-\frac{q^2 R_{cg}^2}{2}\right) \tag{A3}$$

provides preliminary information about the dimensions of cylindrical micelles without the need for fitting detailed models. The modified Guinier equation is an asymptotic expression for $I(q)$ of a collection of cylinders of length L and radius R and is approximately valid for q values between 1/L and 1/R. In this q-range, a plot of ln(qI) versus q^2 is linear, and the slope is proportional to the cross-sectional radius of gyration R_{cg}. For particles with a circular cross-section of radius R, $R_{cg} = R/\sqrt{2}$. For q less than 1/L, ln(qI) is an increasing function of q.

A more complete analysis uses the data over the full q-range to match Eq. A.2. The fitted parameters are the cylinder length and radius (or the ellipsoid semi-major and semi-minor axes) and the prefactor A. A rigorous model for the micelle data would account for the scattering length density difference between the hydrocarbon tails and the hydrophilic head groups. Lecithin-bile salt micelles consist of a hydrophobic "core" of lecithin tails surrounded by a "shell" containing the lecithin head groups and the bile salt. Fitting scattering data from a core-shell cylindrical structure to a constant density model will yield an apparent radius that is a weighted average of the scattering length density distribution (Hjelm et al., 1992; Long, 1993, Long et al., 1994). The fitted micelle length is not affected by the scattering length density distribution. Precise determination of the internal structure requires high quality data at high q where the scattering from the radial cross-section predominates. For the purposes of this paper, it is sufficient to discuss the fitted value of the effective radius in light of previous results (Hjelm et al., 1992; Long, 1993).

The lecithin-bile salt micelle solutions are concentrated, hence $S(q) \neq 1$ at all q due to excluded volume interactions as discussed elsewhere (Long, 1993). For ellipsoidal micelles a "decoupling approximation" can be used to calculate $S(q)$ (Kotlarchyk and Chen, 1983). This expression allows calculation of the effects of interparticle interactions using expressions for $S(q)$

TABLE 4 Shape functions used to fit the SANS data

Shape	$\tilde{P}(q)$*	Fitted parameters
Ellipsoid	$\tilde{P}(q) = 9\int_0^{\pi/2}\left[\frac{j_1(x)}{x}\right]^2 \cos(\beta)\, d\beta \qquad x = q[a^2\sin^2(\beta) + b^2\cos^2(\beta)]^{1/2}$	a = Semimajor axis b = Semiminor axis
Cylinder	$\tilde{P}(q) = \int_0^{\pi/2}\left[\frac{\sin(qH\cos(\beta))2J_1(qR\sin(\beta))}{(qH\cos(\beta))(qR\sin(\beta))}\right]^2 \sin(\beta)\, d\beta$	R = Radius L = Length
Vesicle	$\tilde{P}(q) = \frac{9[\sin(qR) - qR\cos(qR) - \sin(qR_i) + qR_i\cos(qR_i)]^2}{q^6(R^3 - R_i^3)^2}$	R_i = Inner radius = $R - t$ t = Bilayer thickness $P(q) = (\Delta\rho)^2 V^2 \tilde{P}(q)$

* β = angle of orientation, $j_1(x)$ is the first order spherical Bessel function; $J_1(x)$ is the first order Bessel function.

based on the interaction of equivalent spheres. The Random Phase Approximation (RPA) can be used to model the effects of excluded volume interparticle interactions for long cylindrical micelles (de Gennes, 1970, Shimada et al., 1988; Long, 1993). The RPA uses a mean-field approach to describe the interaction potential of an elongated particle with the surrounding particles. Both of these models require an estimate of the particle volume fraction, ϕ. For the calculation of $S(q)$, the particle volume fraction is set equal to the volume fraction of total surfactant in solution assuming the specific volume of the bile salt is 0.75 cm^3/gram (Carey, 1985) and that the anhydrous lecithin molecular volume is 1267 Å^3 (Small, 1967). It is not necessary to consider electrostatic interactions to provide a satisfactory fit to the data.

The model fits to the micelle spectra must not only describe the shape of the spectra with q, but the value of the prefactor A ($= (\Delta\rho)^2\phi V_p$) must be consistent with the known composition of the solution. Ideally, the scattering data would be fit with a core-shell model that would provide the composition of the micelles. This higher resolution analysis has been carried out for L-TDC micelles (Long et al., 1994) with the results that the micelle radius is R = 27 Å (recall that the fitted radius as in Table 2 here is an apparent value), the radius of the hydrocarbon core is R_c = 17 Å, the shell scattering length density is 3.5×10^{10} cm^{-2}, and the core scattering length density is -0.29×10^{10} cm^{-2}. With these parameters the average scattering length density is calculated according to (Glatter, 1982)

$$\bar{\rho} = R^{-2}[\rho_t R_c^2 + \rho_h(R^2 - R_c^2)] \tag{A4}$$

to give $(\Delta\rho)^2 = 1.9 \times 10^{21}$ cm^{-4}. This estimate of the average scattering length density, along with the fitted value of A and the particle length obtained from the fit of $\tilde{P}(q)$, yields the volume fraction of surfactant in the micelles. This volume fraction is the sum of the lecithin and bile salt within the aggregate, and does not include the bile salt that makes up the IMC. The IMC is calculated from the difference between the fitted ϕ_m and the total surfactant volume fraction.

The vesicle solutions are sufficiently dilute that interparticle interactions are negligible, and $I = N_p P(q)$. Fitting the scattering data is complicated, however, by the apparent size polydispersity of the vesicle solutions. The scattered intensity in this case is the average of $P(q)$ over all particle sizes present.

$$I(q) = \langle N_p \rangle \int_0^\infty f(R_i) P(R_i; q)\, dR_i, \tag{A5}$$

where the integration is over the inner radius R_i, $f(R)$ is a size distribution function, and $\langle \cdots \rangle$ indicates the average over all particle sizes. A Schultz distribution is used for the calculations here (Aragon and Pecora, 1976, Kotlarchyk et al., 1988), and

$$f(R) = \frac{1}{\Gamma(z+1)}\left[\frac{(z+1)}{R_{av}}\right]^{z+1} R^z \exp\left[-\frac{(z+1)R}{R_{av}}\right], \tag{A6}$$

with R_{av} equal to the number average of the inner radius, z is an integer width parameter related to the standard deviation σ: $z = R_{av}^2/\sigma^2 - 1$, and $\Gamma(x)$ is the Gamma function. Analytical expressions of the average shape function are possible only if the ratio of the outer to the inner radius remains constant. The integration of Eq. A.5 is performed numerically to accommodate the more physically realistic assumption of constant bilayer thickness.

The fitted parameters for this model are the average inner vesicle radius, the standard deviation, σ, and the bilayer width. It is assumed that the vesicles are made up of lecithin alone with no bile salt, and the bilayer width is held the same for all samples. The contrast between the hydrocarbon tails and the solvent ($(\Delta\rho_c)^2 = 4.4 \times 10^{21}$ cm^{-4}) dominates the scattered intensity, so the head groups make little or no contribution to either the q-dependence or the magnitude of the scattered intensity. Thus, $\langle N_p \rangle = \phi_t \langle V \rangle^{-1}$ where ϕ_t is the volume fraction of the hydrocarbon tails (using a hydrocarbon tail volume of 970 Å^3/lecithin molecule, which was calculated using the expression for the volume of two 17 carbon chains (Tanford, 1980)) and $\langle V \rangle (= 4\pi[R_{av}^2 t(z+2)/(z+1) + R_{av}t^2 + t^3/3])$ is the average vesicle volume.

Size polydispersity has a significant effect on the shape of the scattering spectra around its first maximum. The average vesicle radius dictates the q-position of the first maximum and does not change significantly with variation of the standard deviation. Incorporating the effects of polydispersity dampens the magnitude of the oscillations of the shape factor and improves the overall fit to the data. Smearing of the scattering curves caused by the wavelength spread and detector geometry can cause shallow maxima and minima similar to the effects of polydispersity. These effects were calculated for the instrument geometry of the Oak Ridge spectrometer (Pedersen et al., 1990, Ramakrishnan, 1985, Wignall et al., 1988) and not found to improve these fits over those obtained with the polydisperse vesicle model.

The transition from cylindrical micelles to polydisperse vesicles is a continuous transformation, and there is a range of concentrations over which the two types of aggregates coexist. To model the scattered intensity within this region, $S(q)$ is taken as 1, and the intensity is written as a weighted sum of the intensity of both groups of particles,

$$I(q) = A_m \tilde{P}_m(q) + A_v \tilde{P}_v(q), \tag{A7}$$

where the subscripts m and v indicate micelles and vesicles respectively. The vesicles are modeled using the expressions for a polydisperse dispersion, and $A_v \equiv (\Delta\rho)^2 \phi_v \langle V_v^2 \rangle \langle V_v \rangle^{-1}$. The average of the volume squared comes from the normalization of $\langle P(q) \rangle$ to obtain $\tilde{P}_v(q)$, and is given by

$$\langle V_v^2 \rangle = 16\pi^2 \left[R_{av}^4 t^2 \frac{(z+4)(z+3)(z+2)}{(z+1)^3} + \frac{4}{3} R_{av}^3 t^3 \frac{(z+3)(z+2)}{(z+1)^2} + \frac{5}{3} R_{av}^2 t^4 \frac{(z+2)}{(z+1)} + \frac{2}{3} R_{av} t^5 + \frac{t^6}{9} \right], \tag{A8}$$

where t is the bilayer thickness.

Dynamic light scattering

To compare the results of the analysis of SANS spectra with dynamic light scattering measurements, the translational diffusion coefficients of the surfactant aggregates are estimated using the dimensions derived from the SANS data. For cylindrical micelles with P = L/2R,

$$D_t = kT(\ln(p) + \gamma)/3\pi\eta L \tag{A9}$$

where η is the solvent viscosity and $\gamma = 0.312 + 0.565/p + 0.1/p^2$ (Garcia de la Torre and Bloomfield, 1981). The function γ corrects for differences in the frictional resistance of finite and infinite cylinders.

For polydisperse vesicles, the first cumulant of the autocorrelation function is proportional to the z-averaged diffusion coefficient

$$\langle D \rangle_z = \int f_i(R) P_i(R; q) D_i\, dR \Big/ \int f_i(R) P_i(R; q)\, dR \tag{A10}$$

where $V_i = 4\pi(R^3 - R_i^3)/3$, $P_i(R; q)$ is given in Table A.1, and $f_i(R)$ is the Schultz distribution function (Eq. A.6).

For both the micelles and the vesicles the sphere-equivalent hydrodynamic radius is determined from the calculated diffusion coefficient and Eq. 1 from the text.

REFERENCES

Almog, S., T. Kushnir, S. Nir, and D. Lichtenberg. 1986. Kinetic and structural aspects of reconstitution of phosphatidylcholine vesicles by dilution of phosphotidylcholine-sodium cholate mixed micelles. *Biochemistry.* 25:2597–2605.

Almog, S., B. J. Litman, W. Wimley, J. Cohen, E. J. Wachtel, Y. Barenholz, A. Ben-shaul, and D. Lichtenberg. 1990. States of aggregation and phase transformations in mixtures of phosphatidylcholine and octyl glucoside. *Biochemistry.* 29:4582–4592.

Aragon, S. R., and R. Pecora. 1976. Theory of dynamic light scattering from polydisperse systems. *J. Chem. Phys.* 64:2395–2404.

Bacon, G. E. 1975. Neutron Diffraction. Clarendon, Oxford. 39–41.

Borgström, B. 1978. Equilibrium of taurodeoxycholate between mixed micellar and aqueous phases: effect of amphiphile. *Lipids.* 13: 187–189.

Brouillette, C. G., J. P. Segrest, T. C. Ng, and J. L. Jones. 1982. Minimal

size phosphatidylcholine vesicles: effects of radius of curvature on head group packing and conformation. *Biochemistry.* 21:4569–4575.

Carey, M. C. 1985. Physical-chemical properties of bile acids and their salts. *In* Sterols and Bile Acids. H. Danielsson and J. Sjövall, editors. Elsevier Science B. V., New York. 345–403.

Cornell, B. A., J. Middlehurst, and F. Separovic. 1980. The molecular packing and stability within highly curved phospholipid bilayers. *Biochim. Biophys. Acta.* 598:405–410.

de Gennes, P. G. 1970. Theory of x-ray scattering by liquid macromolecules with heavy atom labels. *J. Physiol. (Paris).* 31:235–238.

Donovan, J. M., N. Timofeyeva, and M. C. Carey. 1991. Influence of total lipid concentration, bile salt: lecithin ratio, and cholesterol content on inter-mixed micellar/vesicular (non-lecithin-associated) bile salt concentrations in model bile. *J. Lipid Res.* 32:1501–1511.

Douglas, C. B., and E. W. Kaler. 1991. Phase behavior of aqueous mixtures of hexaethylene glycol monododecyl ether and sodium alkylsulfonates. *Langmuir.* 7:1097–1102.

Duane, W. 1975. The intermicellar bile salt concentration in equilibrium with the mixed-micelles of human bile. *Biochim. Biophys. Acta.* 398: 275–286.

Duane, W. C. 1977. Taurocholate- and taurochenodeoxycholate-lecithin micelles: the equilibrium of bile salt between aqueous phase and micelle. *Biochem. Biophys. Res. Commun.* 74:223–229.

Garcia de la Torre, J., and V. A. Bloomfield. 1981. Hydrodynamic properties of complex, rigid, biological macromolecules: theory and applications. *Q. Rev. Biophys.* 14:81–139.

Glatter, O. 1982. Interpretation. *In* Small Angle X-Ray Scattering. O. Glatter and O. Kratky, editors. Academic, New York. 167–196.

Groen, A. K., R. Ottenhoff, P. L. M. Jansen, J. van Marle, and G. N. J. Tytgat. 1989. Effect of cholesterol nucleation-promoting activity on cholesterol solubilization in model bile. *J. Lipid Res.* 30:51–58.

Hjelm, R. Jr. 1985. The small-angle approximation of x-ray and neutron scatter from rigid rods of non-uniform cross section and finite length. *J. Appl. Cryst.* 18:452–460.

Hjelm, R. P. Jr., P. Thiyagarajan, and H. Alkan. 1988. A small-angle neutron scattering study of the effects of dilution on particle morphology in mixtures of glycocholate and lecithin. *J. Appl. Cryst.* 21:858–863.

Hjelm, R. P., M. H. Alkan, and P. Thiyagarajan. 1990. Small-angle neutron scattering studies of mixed bile salt-lecithin colloids. *Mol. Cryst. Liq. Cryst.* 180A:155–164.

Hjelm, R. P., P. Thiyagarajan, and M. H. Alkan-Onyuksel. 1992. Organization of phosphatidylcholine and bile salt in rodlike mixed micelles. *J. Phys. Chem.* 96:8653–8661.

Hofmann, A. F., and K. J. Mysels. 1988. Bile salts as biological surfactants. *Colloids Surf.* 30:145–173.

Koppel, D. E. 1971. Analysis of macromolecular polydispersity in intensity correlation spectroscopy: the method of cumulants. *J. Chem. Phys.* 57: 4814–4820.

Kotlarchyk, M., and S.-H. Chen. 1983. Analysis of small angle neutron scattering spectra from polydisperse interacting colloids. *J. Chem. Phys.* 79:2461–2469.

Kotlarchyk, M., R. B. Stephens, and J. S. Huang. 1988. Study of Schultz distribution to model polydispersity of microemulsion droplets. *J. Phys. Chem.* 92:1533–1538.

Kratky, O. 1982. Natural high polymers in the dissolved and solid state. *In* Small Angle X-Ray Scattering. O. Glatter and O. Kratky, editors. Academic, New York. 361–386.

Lee, S. P., H. Z. Park, H. Madani, and E. Kaler. 1987. Partial characterization of a non-micellar system of cholesterol solubilization in bile. *Am. J. Physiol.* 252:G374-G383.

Lichtenberg, D., Y. Zilberman, P. Greenzaid, and S. Zamir. 1979. Structural and kinetic studies on the solubilization of lecithin by sodium deoxycholate. *Biochemistry.* 18:3517–3525.

Little, T. E., H. Madani, S. P. Lee, and E. Kaler. 1993. Lipid vesicle fusion induced by phospholipase C activity in model bile. *J. Lipid Res.* 34: 211–217.

Long, M. A. 1993. Characterization of surfactant aggregates in bile using small-angle scattering. Ph. D. thesis. University of Delaware. 222 pp.

Long, M. A, E. W. Kaler, S. P. Lee, and G. D. Wignall. 1994. Characterization of lecithin-taurodeoxycholate mixed micelles using small angle neutron scattering and static and dynamic light scattering. *J. Phys. Chem.* 98:4402–4410.

Marignan, J., J. Appell, P. Bassereau, G. Porte, and R. P. May. 1989. Local structures of the surfactant aggregates in dilute solutions deduced from small angle neutron scattering patterns. *J. Phys. France.* 50:3553–3566.

Mazer, N. A., G. B. Benedek, and M. C. Carey. 1980. Quasielastic light-scattering studies of aqueous biliary lipid systems *Biochemistry.* 19: 601–615.

Mazer, N. A., P. Schurtenberger, M. Carey, and R. Preisig. 1984. Quasielastic light scattering studies of native hepatic bile from the dog: comparison with aggregative behavior of model biliary lipid systems. *Biochemistry.* 23:1994–2005.

Müller, K. 1981. Structural dimorphism of bile salt/lecithin mixed micelles. *Biochemistry.* 20:404–414.

Nichols, J. W., and J. Ozarowski. 1990. Sizing of lecithin-bile salt mixed micelles by size-exclusion high-performance liquid chromatography. *Biochemistry.* 29:4600–4606.

Pedersen, J. S., D. Posselt, and K. Mortensen. 1990. Analytical treatment of the resolution function for small-angle scattering. *J. Appl. Cryst.* 23: 321–333.

Porod, G. 1982. General theory. *In* Small Angle X-Ray Scattering. O. Glatter and O. Kratky, editors. Academic, New York. 17–51.

Ramakrishnan, V. 1985. A treatment of instrumental smearing effects in circularly symmetric small-angle scattering. *J. Appl. Cryst.* 18:42–46.

Reda, F., and C. Spink. 1987. Dinaphthylpropane as a probe of the behavior of bile salt-lecithin mixtures. *J. Phys. Chem.* 91:1628–1634.

Rotenberg, M., and D. Lichtenberg. 1991. What determines the size of phospholipid vesicles made by detergent-removal techniques. *J. Colloid Interface Sci.* 144:591–594.

Schubert, R., and K.-H. Schmidt. 1988. Structural changes in vesicle membranes and mixed micelles of various lipid compositions after binding of different bile salts. *Biochemistry.* 27:8787–8794.

Schurtenberger, P., N. Mazer, and W. Känzig. 1985. Micelle to vesicle transition in aqueous solutions of bile salt and lecithin. *J. Phys. Chem.* 89:1042–1049.

Shankland, W. 1970. The equilibrium and structure of lecithin-cholate mixed micelles. *Chem. Phys. Lipids* 4:109–130.

Shimada, T., M. Doi, and K. Okano. 1988. Concentration fluctuation of stiff polymers. I. Static structure factor. *J. Chem. Phys.* 88:2815–2821.

Small, D. M. 1967. Phase equilibria and structure of dry and hydrated egg lecithin. *J. Lipid Res.* 8:551–557.

Stark, R. E., G. J. Gosselin, and J. M. Donovan. 1985. Influence of dilution on the physical state of model bile systems: NMR and quasi-elastic light-scattering investigations. *Biochemistry.* 24:5599–5605.

Stark, R. E., J. L. Manstein, W. Curatolo, and B. Sears. 1983. Deuterium nuclear magnetic resonance studies of bile salt/phosphatidylcholine mixed micelles. *Biochemistry.* 22:2486–2490.

Szleifer, I., A. Ben-Shaul, and W. M. Gelbart. 1987. Statistical thermodynamics of molecular organization in mixed micelles and bilayers. *J. Chem. Phys.* 86:7094–7109.

Tanford, C. 1980. The Hydrophobic Effect. John Wiley and Sons, New York.

Vinson, P. K., Y. Talmon, and A. Walter. 1989. Vesicle-micelle transition of phosphatidylcholine and octyl glucoside elucidated by cryo-transmission electron microscopy. *Biophys. J.* 56:669–681.

Walter, A., P. K. Vinson, A. Kaplun, and Y. Talman. 1991. Intermediate structures in the cholate-phosphatidylcholine vesicle-micelle transition. *Biophys. J.* 60:1315–1325.

Wignall, G. D., D. K. Christen, V. Ramakrishnan. 1988. Instrumental resolution effects in small-angle neutron scattering. *J. Appl. Cryst.* 21: 438–451.